

Peter A. Bandettini, Ph.D.

fMRI Connectivity, Hemodynamics, and Contrasts

Section on Functional Imaging Methods, Laboratory of Brain and Cognition, NIMH

Section 1: Introduction.....	2
Executive Summary.....	2
Significance, Innovation Appropriateness to Intramural Environment.....	3
Section 2: Research Themes.....	4
Theme 1: Fluctuations and Connectivity in fMRI.....	4
1A. Introduction: Connectivity Information.....	4
1B. Past studies.....	5
1B-1. Connectivity Based Brain Reading.....	5
1B-2. Multi-echo EPI with Cardiac Gating.....	6
1C. Current Studies.....	8
1C-1. Classifying distraction using Magnitude and Connectivity Changes.....	8
1C-2. Brain State Classification Success is Independent of Segmentation Approach.....	9
1C-3. From Classification to Spatial Localization.....	9
1C-4. Magnitude vs Connectivity Locations.....	10
1C-5. Resting state Frequency Signatures across Cortical Regions.....	11
Theme 2: Pushing the limits of Hemodynamic stability, sensitivity and specificity.....	12
2A. Introduction: What more can we extract from hemodynamics?.....	12
2B. Past studies.....	13
2B-1. Whole brain activation at 7T.....	13
2B-2. Multi-Echo EPI for slow change assessment.....	14
2C. Current Studies.....	15
2C-1. Layer specific mapping in sensory and motor cortex at 7T using VASO.....	15
2C-2. Multi-echo EPI and improvements on massive trial repetition.....	16
2C-3. Cross-run correlation improvements with multi-echo EPI.....	17
Theme 3: Novel Contrast and Interventions.....	18
3A. Introduction: Expanding the utility of fMRI and MRI.....	18
3B. Past Studies.....	18
3B-1: Structural MRI changes with learning and exercise.....	18
3C. Current Studies.....	19
3C-1. Iron deposition in basal ganglia increases with fitness.....	19
3C-2: Exploring Valsalva-induced changes using VASO.....	20
3C-3: Blood Volume fMRI with 3D-EPI-VASO: any benefits over SMS-VASO?.....	21
3C-4: Fast Dynamic Measurement of Functional T1 and Gray Matter Thickness.....	21
List of SFIM Publications since last BSC report.....	23
Resource Sharing and Data Sharing.....	27
Collaborations.....	27
Resources Requested.....	28
Bibliography.....	29

Section 1: Introduction

Executive Summary

The research carried out by the Section on Functional Imaging Methods (SFIM) is aimed to deepen and broaden the understanding and utility of fMRI and MRI. For over 17 years that the Unit-then-Section on Functional Imaging Methods (SFIM) has existed, our primary goal has been to extract as much usable neuronal and physiologic information as possible from the fMRI and MRI signal. More recently, we have been actively working to translate this understanding into methodology that directly impacts basic research and clinical practice. Most of our 37 papers published since the last report reflect these directions. The strength of SFIM is that our work spans the interface of contrast mechanism research, methodology development, and clinical and basic neuroscience applications of fMRI. We believe that the best innovations are driven by the needs of specific applications and that the best and most innovative applications are those that use the latest and best methodology. Our research and the expertise of members of SFIM strike this balance between contrast mechanism, methodology, and applications research.

Our research can be categorized into three themes. The first is “Fluctuations and Connectivity in fMRI.” The second is “Pushing the limits of Hemodynamic Stability, Sensitivity, and Specificity.” The third is “Novel Contrast and Interventions.”

Theme 1: After about a decade of quiescence since the inception of resting state fMRI (rsfMRI) in 1995[1], the field has been growing rapidly. Temporal correlations in spontaneous fluctuations across brain regions are commonly interpreted as an indicator of functional connectivity (FC). While these patterns of connectivity follow known functional architecture, they vary with population, individual subject, task, and mental state - and are constantly changing across time scales from seconds to days. The resting state signal clearly contains meaningful information yet we don’t fully understand its information content, neural underpinnings, variability, or even its functional purpose. The field is currently in an explosive growth phase as many groups, including SFIM are working to better understand this signal and to develop better methods to extract, quantify, and compare it. Our work in Theme 1 has aimed to improve brain state classification methods in individuals, to track ongoing cognition and attention, and generally to better understand how rsfMRI varies. Ultimately, a major clinical goal is to use this signal on an individual basis in order to help diagnose, treat, and predict outcome of individuals in a clinical setting.

Theme 2: A central theme in SFIM over the years has continued to be understanding and expanding the limits of what the activation-induced hemodynamic response can provide in terms of neuronal and physiologic information. We have been working to increase temporal stability as well as to push back the limits of functional spatial and temporal resolution. We have followed up on our past work on massive averaging and model free analysis with a study at higher field strength that involved modulation of cognitive load. We have continued our work developing multi-echo EPI approaches for increased time series stability. With the arrival of a new post doc, Laurentius Huber, we are very excited to have begun very high resolution mapping of layer dependent fMRI activation and connectivity in sensory and motor cortex - towards the goal of using fMRI to infer feedback vs feedforward connections from layer-specific activity.

Theme 3: The focus of this last theme is our continued effort to explore beyond “standard” fMRI or MRI with novel pulse sequences, interventions, or contrasts. In the past decade we have sought, for example, to develop neuronal current imaging[2] to characterize anatomic changes with chronic interventions[3], and to test novel methods to calibrate the fMRI signal such as with the Valsalva maneuver[4] or using ongoing resting state fluctuations[5]. We have continued this exploration, innovation,

and development along these lines with research to characterize and understand anatomic changes with exercise[6], fast T1 changes with a task, and blood volume changes with the Valsalva maneuver.

During the past four years SFIM has produced a body of novel work that includes not only further development and testing of methods that we have previously introduced but also high risk, high gain work that is forging new directions. An example of the former is our substantial body of work establishing the advantages and limits of multi-echo EPI. Examples of the latter are our resting state layer dependent fMRI mapping and our correlation-based task decoding methodology development. In the last BSC report, we emphasized the need to move to individual subject classification. Individual classification involves either categorizing a subject as belonging to a specific population or deriving usable information on the individual's functional organization or ongoing brain activity during a scan session. All of the studies in this report are individual subject studies.

This report is organized as follows: The themes are numbered 1 through 3. Within each theme, there are three sub headings: A is a brief introduction; B is the progress report which describes projects that have been completed and published after December of 2012 - called Past Studies; and C describes ongoing projects that have only been published in abstract form - called Current Studies. We do not discuss projects that are only in the conceptual stage. At the end of each project description, the section members and collaborators are listed in parentheses in alphabetical order, with the primary investigator in bold print. Collaborators outside of SFIM are in red.

Significance, Innovation, and Appropriateness to the Intramural Environment

The field of fMRI is over a quarter century old and by all measures, it has been advancing at an accelerating rate in the past 5 to 10 years. This accelerated advancement is largely due to the improvement in our understanding of - and confidence in - the fMRI signal as well as rapid growth in the sophistication in methodology. Methods, understanding, and advanced applications drive the field. The research of SFIM is focused directly on these areas. The cutting edge innovations come from close collaborations of more technically focused researchers and those focused on applications. The NIH intramural program has a critical mass of both neuroimaging methods and applications researchers. Extramural funding for methods development has been relatively sparse, with a few notable exceptions, including the Human Connectome Project and the BRAIN Initiative. While these investments are starting to pay off substantially, re-energizing the field of fMRI and brain mapping in general, the intramural environment has offered the right balance of stability as a rich environment for technically savvy collaborators who are able to "beta-test" for some of the latest innovations coming from SFIM as well as the Functional MRI Core Facility.

Our most significant papers over the years have helped to pioneer new processing methodologies and a deeper understanding of the hemodynamic response. These papers have introduced advances that include: simultaneous perfusion and BOLD imaging[7], multivariate pattern effect analysis[8], ongoing brain state (or task) decoding based on connectivity[9], spatial heterogeneity of resting state dynamics[10], respiration contribution to resting state fluctuations[5], periodic interaction of resting state networks[11], high resolution layer dependent resting state and activation mapping, entire brain activation mapping with massive averaging[12], the rationale for *not* performing global regression[13], optimal event related timing[14], motion-decoupled fMRI removing task correlated movement[15], BOLD temporal nonlinearities[16], pushing temporal resolution by task modulation and hemodynamic response characterization[17], direct neuronal current imaging in cell cultures[2], and of course, perhaps our most

successful method to penetrate the field: multi-echo EPI for time series cleanup[18, 19] and automated segmentation based on multi-echo EPI data.

Currently, a central goal - perhaps the primary goal - of the field is the application of fMRI to *individual* subjects. Since the very beginning of fMRI, we have been able to see activation-related signal changes from individuals but lacked the sensitivity and processing sophistication to classify individuals based on their spatial and temporal patterns of resting state or task-related activity. One could see the visual cortex or motor cortex light up but could not, for example, derive information about the subject's intelligence, musical talent, or likelihood for that subject to suffer from schizophrenia later in life. Recently, because of a combination of massive databases with corresponding genetic and behavioral data, better characterization of cross subject variability, improved methods for cleaning up the fMRI signal, and, importantly, better machine learning approaches tailored to neuroimaging data, the field is starting to make more rapid progress in uncovering subtle yet usable fMRI-based biomarkers for characterizing individual subjects. This quest will define the next decade of fMRI method development, and the work of our group is well positioned, along with our fMRI Core Facility with our new Data Sharing and Machine Learning Teams, to make fundamental scientific and methodological contributions along these avenues.

Section 2: Research Themes

Theme 1: Fluctuations and Connectivity in fMRI

1A. Introduction: *Connectivity Information*

The subfield of resting state fMRI-based connectivity mapping is rapidly evolving. Resting state fMRI has proven to be a high-fidelity and highly reproducible method to discern differences in groups, individuals, and brain regions. The resting state signal is also proving to be a rich source of research as we are just beginning to understand its dynamics and variability as well as its neural and behavioral correlates. We are at just the beginning of merging advanced acquisition methods, pre- and post-processing methods, and carefully crafted neuroscience and clinical paradigms to fully exploit this information-rich signal. The research of SFIM has devoted considerable resources to the study of resting state connectivity and, specifically, dynamic resting state connectivity.

In one study, we applied sliding window pairwise connectivity analysis to successfully differentiate and track four different ongoing tasks [9]. This was the first of its kind to decode ongoing function from measures of connectivity rather than magnitude. From this initial study, several new questions arose. The informative connectivity changes appeared from regions that were more extensive than known areas of magnitude changes - potentially revealing informative signal changes that are typically missed when assessing magnitude changes alone. This observation also has dovetailed with our previous finding using massive averaging and a model free exploration of activation - also revealing nearly all the gray matter activated in some manner even during a simple task[12]. We followed this initial finding with a study involving attention shifts in the scanner and found that dynamic magnitude changes and connectivity changes carried different information related to whether the subject was internally or externally distracted.

One fundamentally important issue related to our approach was a question related to the initial segmentation of the brain to determine the time series on which to perform sliding window pairwise correlation analysis. We found that if dimensionality reduction (i.e. principle component analysis (PCA)) was performed following time series extraction from each segment and before sliding window pairwise

correlation analysis, the initial segmentation scheme was not a significant determinant of the effectiveness of the decoding of ongoing task - thus allowing arbitrary segmentation as a first step. This new finding frees up a degree of latitude in comparing resting state connectivity across individuals as precise registration and segmentation may not be a critical step.

Ongoing research from SFIM in this theme includes addressing the question of how to move back and forth between a signal that was optimized for “decoding” or classification of a task and the spatial origins of this signal. To bring fMRI decoding to full use, a clear transformation between decoding information and spatial mapping is critical. We are also collaborating with Dr. Eric Wong from UCSD to develop and implement a pulse sequence that collects extremely sparse data that approximately matches the spatial resolution of a typically segmented brain for dynamic connectivity analysis (150 to 500 segments) [20]. Collecting this data as a first step saves considerable time and substantially boosts signal to noise. Lastly, we have begun to work to more precisely characterize power-spectra differences between known functional networks as this information may help characterize individuals and give insight into the functional correlates of resting state fluctuations.

1B. Past Studies

1B-1. Connectivity-based brain reading.

Functional connectivity (FC) patterns in fMRI exhibit dynamic behavior on the scale of seconds[10] with rich spatiotemporal structure and limited number of whole-brain, quasi-stable FC configurations or states recurring across time and subjects. Although several groups have hypothesized that these FC states relate to on-going cognition, and that their quantification may have clinical relevance, evidence of a direct relationship between FC states and on-going cognition has been missing. To fill this gap, we conducted experiments in which we scanned subjects continuously for 25 minutes as they performed and transitioned between 4 different mental states dictated by tasks (i.e., math, 2-back, visual attention, and rest) in blocks of 3 minutes. After appropriate pre-processing we computed FC states for windows ranging from 22.5s to 180s in length. We then submitted these FC states to a clustering algorithm and evaluated whether or not FC states grouped according to mental states. For subjects that performed the tasks consistently, the algorithm was able to group FC states according to mental states almost perfectly for all window durations (Figure 1A). This was not the case for subjects with low and (Figure 1B). This first result suggests

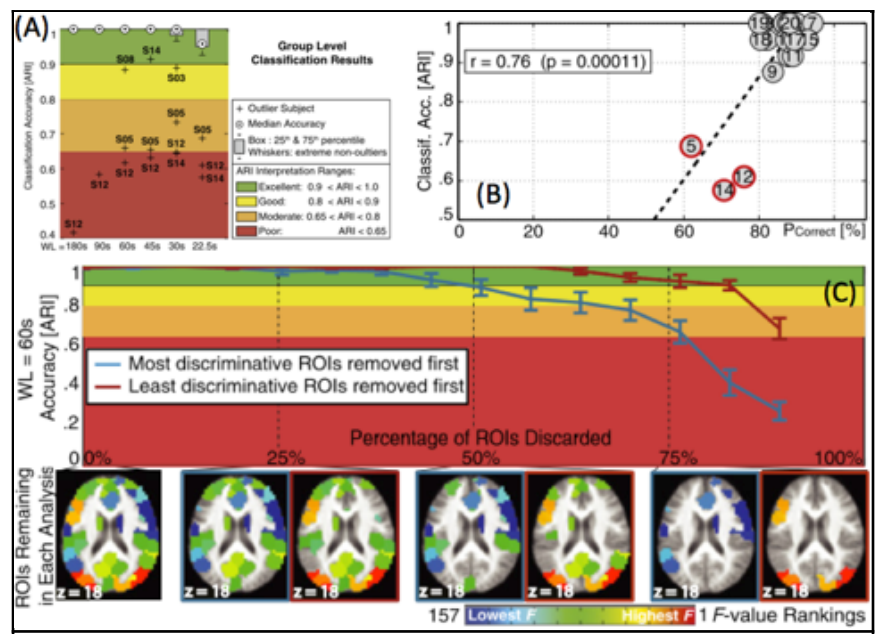


Figure 1: A) Accuracy of state assessment vs window length. B) Correspondence of subject performance (x-axis) to assessment accuracy (y-axis). C) Accuracy as a function of ROI removal. Even with only 50% of the most discriminative ROI's remaining, the accuracy was 90%.

that short-term (<30sec) fluctuations in fMRI connectivity patterns can be reliably used to track ongoing cognition, on an individual subject basis, despite the noisy and indirect nature of BOLD signals as a marker of neuronal activity.

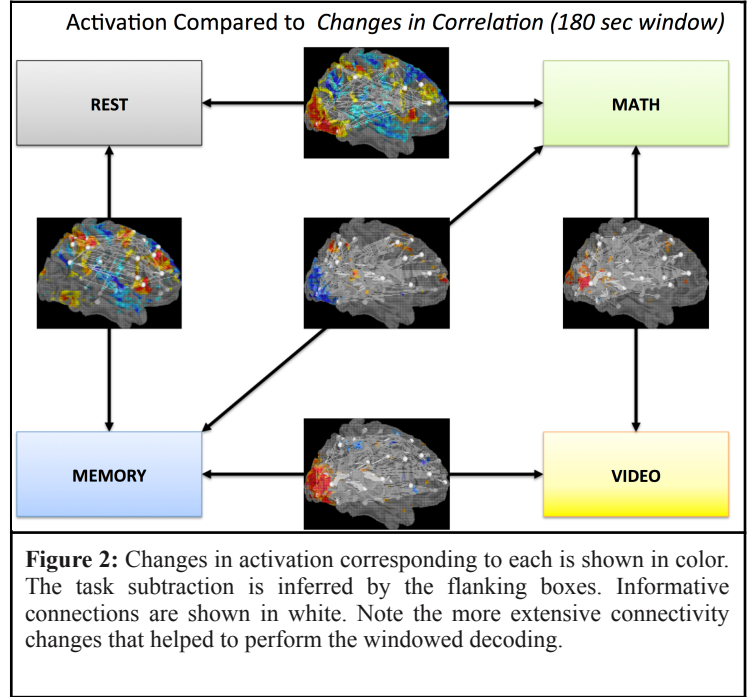
We then conducted additional analyses to determine the spatial distribution of the most informative connections. For this, we sorted regions of interest (ROIs) according to how well they differentiated the tasks in terms of activation levels. We then tested FC states classification using progressively smaller sets of ROIs. In one analysis, we removed the most task-discriminative ROIs first. In a second analysis, we removed ROIs in the opposite order (least task-discriminative first). Independent of window length or exclusion order, classification accuracy decreases monotonically as the number of discarded ROIs increases (Figure 1C). The rate of decrease in accuracy is faster when most discriminative ROIs are removed first, yet removal of a limited set of least discriminative ROIs can also degrade classification. This result, along with that shown in Figure 2 suggests that an FC state is better described by the state of wide spread connections across the brain, rather than by the considerably smaller set of connections between regions whose overall activity changes the most across the tasks under study.

The strong correspondence between FC states and mental states reported here suggests that the detailed study of FC states may provide novel insights into system-level behaviors of the human brain. This work was reported in PNAS[9]. {P. A. Bandettini, L. C. Buchanan, J. Gonzalez-Castillo, D. A. Handwerker, C. W. Hoy, M. E. Robinson, Z. S. Saad}

1B-2. Multi-echo EPI with cardiac gating

Performing BOLD-fMRI studies that target regions such as the brainstem that are surrounded by large vascular structures is particularly difficult given their elevated levels of noise associated with pulsatile motion from normal cardiac function. Certainly enough averaging can reduce the effects of pulsatile motion but another way to minimize it is to acquire images always at the same point within the cardiac cycle (i.e. cardiac-gated imaging); therefore the subcortical units, which are quite small and can move in and out of a voxel with each cardiac cycle, will always remain in the same location.

Irregular repetition times (TR's) resulting from a variable heart rate produce artifactual baseline signal shifts due to T1 relaxation. Guimaraes et al. [21] previously proposed a model-driven approach to account for these artifactual baseline shifts - requiring keeping track of the TR's for each run. Given the non-BOLD nature of the pulsation artifacts and movement that accompanies cardiac-gated acquisitions, we hypothesized that combining cardiac-gated acquisition strategies with multi-echo independent component



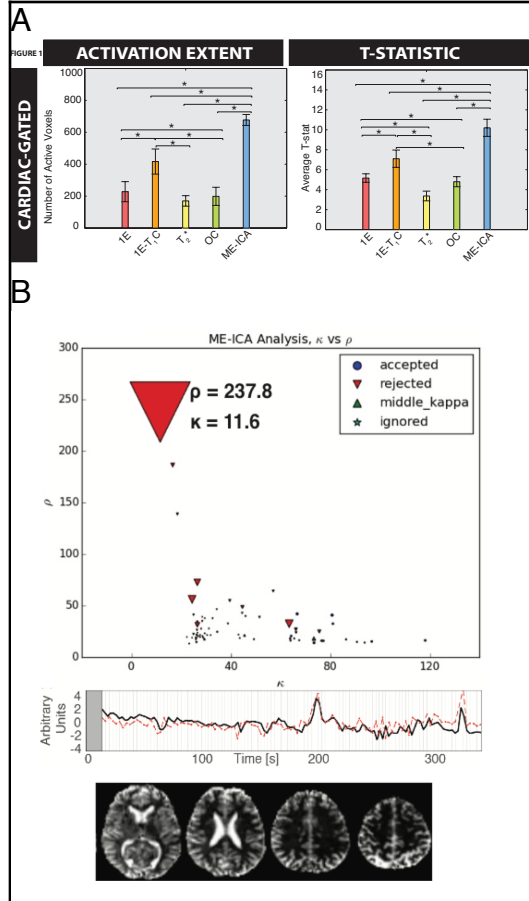


Figure 3. A. Activated voxels in the brain stem region to an auditory stimulation vs time series imaging strategy. B. Non-BOLD intercept change (ρ) vs. BOLD fit (κ) shows the largest (largest magnitude) rejected effect is the T1 effect that maps out to the T1 weighted images at the bottom. The time courses show the close correspondence between the rejected ICA time course and a model based on the TR and a T1 estimate.

needed when gating as the T1 noise, manifest as an ICA component that is non-BOLD, is easily removed.

This approach also suggests the potential of ME-ICA to identify and remove other T1 artifacts such as inflow effects in constant TR acquisitions, that are otherwise difficult to model and account for in a time series.

One more advantage of this approach is that a spatially and temporally registered T1 map falls out as an “artifact” ICA component. This map can be useful for gray matter segmentation. Overall, while this approach is not essential for imaging function in small structures subject to movement with cardiac pulsation, it creates high quality maps much more easily and quickly than standard approaches. Another area that would benefit from this is the spinal cord due to high CSF pulsatility in this area. This study is currently in press in NeuroImage. {P. A. Bandettini, J. A. Derbyshire, L. C. Buchanan, C. Caballero-Gaudes, J. Gonzalez-Castillo, D. A. Handwerker, S. Inati, D. C. Jangraw, P. Panwar, Z. Valentinos, V. Roopchangsingh}

analysis (ME-ICA) based denoising[19] might constitute a powerful approach for the study of the brainstem with fMRI.

To test this hypothesis we acquired cardiac-gated multi-echo fMRI data while 5 subjects performed an auditory task. An auditory task was chosen to activate the inferior colliculus (IC; which sits at the back of the brainstem). Five pre-processing strategies were evaluated: single-echo ignoring the T1 artifact(1E - in Figure 3A); single-echo combined with a model-driven T_1 -baseline correction[21]; dual-echo ratio approach[22], optimal combination of three echoes [23] and ME-ICA[18].

Figure 3B shows ME-ICA always found a noise component (Figure 3B) with high rho (non-BOLD index) and low kappa (BOLD-index) whose time-series heavily correlated with modeled T_1 -baseline shifts based on TR recordings (Figure 3B time series: red=T1-shift model, black=ICA time series), and whose spatial maps clearly delineate gray and white matter based on T_1 differences. The size of the points on the curve delineate the relative contribution to time series noise. As can be seen, the T1-variation point dominates the noise.

A comparison of activation maps produced using the imaging strategies is shown in Figure 4. While gating with TR model-based T_1 correction does produce activation in IC (top right activation map in Figure 4) the more robust results are produced either using ME-ICA without gating or with gating. No T_1 correction is

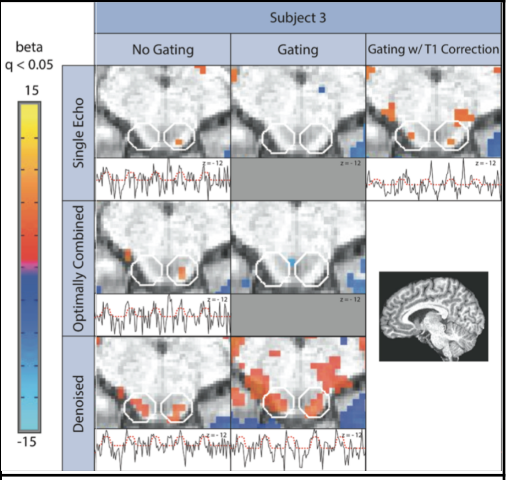


Figure 4. Comparison of activation in Inferior Colliculus. ME-ICA Denoised activation is most clear - and no model based T_1 correction is necessary as the cardiac ICA component is removed automatically based on a low fit to the BOLD TE dependence curve.

1C. Current Studies

1C-1. Classifying Distraction using Magnitude and Connectivity Changes

We have started using the approach described in 1B-1 to develop an objective, continuous metric of sustained attention that is valid for a naturalistic task. In this study, we leverage recent work showing the predictive potential of functional connectivity (FC) in classifying cognitive state[9]. We extract features of interest from changes in both fMRI magnitude as well as FC, and we build a machine learning classifier that uses these features to identify the presence of, and attention to, the auditory distractions in the task.

Eight healthy adults each read text for 4-6 runs, with 30 9-line pages of text per run. On each page, either white noise or unrelated speech was played through headphones. Before each session, subjects were instructed to ignore the speech and focus on the reading (“ignore speech trials”) or attend to both (“attend speech trials”). Multi-Echo fMRI data were acquired during each session, and gaze data were collected using an infrared tracker. After pre-processing the data and applying multi-echo ICA denoising [18], we extracted features that could be used to distinguish white noise from speech trials or attend speech from ignore speech trials. The mean time-course in each ROI in a 200-ROI atlas[24] was extracted, and Support Vector Decomposition (SVD) was used for dimensionality reduction. The remaining component time-courses became the magnitude “Mag” features used in classification. The correlations between ROI components in a 20-s sliding window were calculated and passed through dimensionality reduction to find the “FC” features. The features were sampled once per page and normalized. Logistic regression classifiers were built to classify (1) white noise trials vs. speech trials and (2) focus vs. split trials. In each case, classifiers were trained using (1) only Mag features, and (2) only FC features. The area under the ROC curve (AUC) during leave-one-out cross-validation was used as a figure of merit.

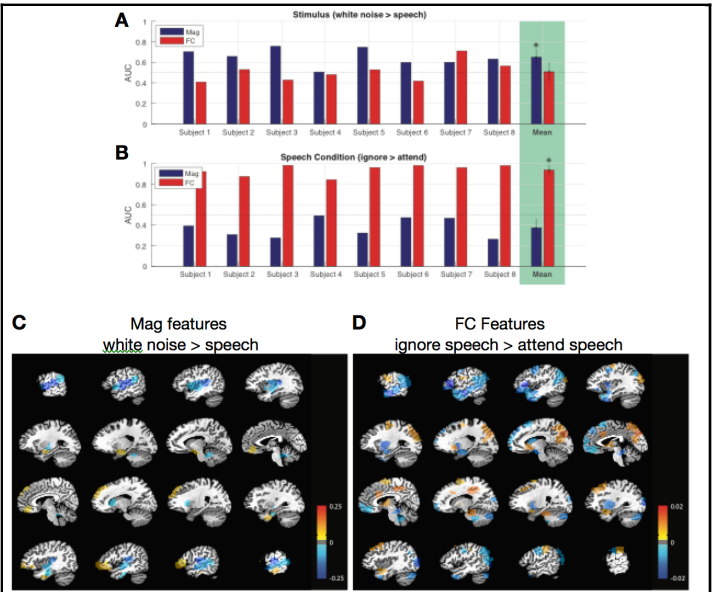


Figure 5: A) Use of magnitude features is superior for detection of stimulus characteristics. B) Use of connectivity features is superior for detection of internal distraction. C and D are the locations of the most informative features.

The results are shown in Figure 5. When classifying white noise vs. speech, Mag features were effective and FC features were not. When classifying ignore speech vs. attend speech trials, however, FC features greatly outperformed Mag features, reaching an unusually high mean AUC value of 0.94. To localize predictive features, we calculated forward models (FM), which can be interpreted as the coupling between the original data and the classifier output. The Mag FM's illustrate that lower fMRI magnitude in temporal cortex provided evidence for white noise trials. The FC FM's illustrate that evidence for ignore speech trials came from a different set of regions including temporal cortex and precuneus (increased FC) and the OFC and ventral striatum (decreased FC). Such FC patterns may provide an effective, objective

metric of sustained attention on a single-trial level in educational scenarios. This could pave the way for fMRI-based evaluations, interventions, or real-time feedback that could help readers – especially those with attention-related disorders – to better resist distraction and control attentional state. *{P. A. Bandettini, J. Gonzalez-Castillo, D. A. Handwerker, D. C. Jangraw, P. Panwar, V. Zachariou}*

1C-2. Brain state classification success is independent of segmentation approach.

Recent work has illustrated the power of functional connectivity patterns to provide information about the task being performed[9]. This technique relies on a parcellation of the brain into ROIs, generally determined a priori from anatomical boundaries or resting state connectivity patterns. Once the time-course of activity in each ROI is determined, pairs are correlated using a sliding window approach. Finally, a dimensionality reduction step–typically singular value decomposition (SVD) – is performed to remove noise, thus aggregating connectivity patterns across the whole brain. In this study, we evaluate the ability of the dimensionality reduction step to extract informative patterns when the original parcellations are less rigidly determined, opening up the possibility of extracting these informative FC features in real time.

A newly proposed imaging sequence may make it possible to record activity from predetermined ROIs directly[20], removing the need for voxel-wise pre-processing and averaging, which can be computationally expensive. This speedup could clear the way for rapid calculation of FC features, which have proven highly informative. This, in turn, could lead to real-time decoding and feedback based on these signals. If the exact regions in the parcellation are unimportant, we could parcel in-brain voxels randomly and count on recovering the informative patterns in the dimensionality reduction step.

To test the plausibility of this approach, we constructed random (but still contiguous) parcellations of roughly equal size using an algorithm from Craddock et al. [24] and repeated the process of task clustering detailed by Gonzalez-Castillo et al.[9], using the same data. The results demonstrated that the clustering algorithm performs just as well with the random parcellations as it did with the connectivity-based atlas as shown in Figure 6. Future work will explore the impact of other changes that could simplify or streamline the proposed imaging sequence, such as overlapping or non-contiguous ROIs. *{P. A. Bandettini, J.Gonzalez-Castillo, D. C. Jangraw}*

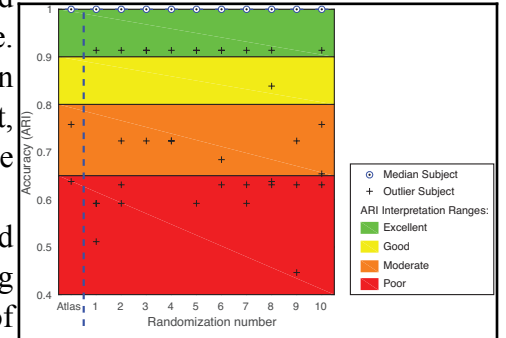


Figure 6: The accuracy of the clustering algorithm was evaluated using the adjusted rand index (ARI), showing the ability of the algorithm to group time windows together that were in the same task. The output for each subject using the standard atlas is compared to 10 randomizations. For all randomizations, the median subject had perfect groupings, with a small number of outliers.

1C-3. From Classification to Spatial Localization

Recent work has demonstrated the powerful ability of FC patterns to identify individuals as belonging to a specific group or having a specific behavioral trait, however, these FC patterns also change with the subject’s task or attentional state in a highly reproducible way. In spite of the success of these classification studies, the spatial origins of the activity that produced these patterns are difficult to visualize and study, and are therefore largely unexplored. In this study, we seek ways to map informative FC patterns back onto the regions and time points that produced them, allowing a more thorough exploration of these highly informative signals.

We used synthetic data to illustrate the feasibility of our approach, which we call “discriminative signal enhancement” shown in Figure 7. We generated activity for a set of 4 ROIs with distinct patterns of connectivity during 2 conditions of a block design task. Once a classifier was built to distinguish trials in the two blocks based on these FC patterns, we used the weights and connectivity patterns to find times when each ROI pair contributed useful information to the classifier. At times when a pair’s connectivity was informative, we gave higher weights to both ROI’s in that

pair. In the synthetic data, this method successfully highlighted the activity in informative regions at the times when their FC with another region was useful to the classifier.

Future work will use data from existing SFIM paradigms that feature dynamic FC changes to leverage a classifier into a map of the original activity that informed it. This exploratory tool will help generate new hypotheses for a more detailed study of these important patterns. {P. A. Bandettini, J. Gonzalez-Castillo, D. C. Jangraw}

1C-4. Magnitude vs. Connectivity Locations

Prior work from SFIM has demonstrated that: (1) overly strict response models combined with limited TSNR result in incomplete maps of brain function[12]; and (2) that functional connectivity based task decoding improves when connectivity between areas not rendered as significantly active in traditional activity-based analyses are considered during the analyses[9]. It then follows that functional connectivity may provide higher sensitivity for detecting regions involved in a task—relative to traditional magnitude based analyses—given its multivariate nature and lack of assumptions regarding expected hemodynamic response shape. We are currently conducting new analyses to evaluate the potential benefits of connectivity-based brain mapping relative to traditional magnitude-based approaches. In particular, preliminary work will focus on the empirical evaluation of the following set of working hypotheses:

H1. If tasks reliably modulate activity in areas not commonly detected with traditional GLM-based approaches, BOLD task-based datasets should contain connections between regions of no a-priori relationship with the task whose connectivity strength remains reliably constant across repetitions of the task.

H2. The spatial distribution and strength of such reliable connections should vary in a meaningful manner across different tasks.

H3. Connectivity-based decoding accuracy should degrade when such reliable connections with no-task fluctuations are discarded in a manner similar to how it happens when connections involving regions of primary relationship to the task are eliminated from the analysis.

Analysis of the multi-task runs originally collected for 1B-1 (Figure 1) provides initial confirmation for H3.

Moreover, initial analyses on a previously acquired dataset in which we collected 100 functional runs in individual subjects performing a visual stimulation plus simple attention control task suggests that H1 is also valid. Figure 8 shows how connections with reliable strength values across the 100 runs ($\text{CVAR} < 0.3$) are widely distributed throughout the entire cortex, extending well beyond primary visual cortex.

As mentioned in the introduction to this report, we feel that, if confirmed, this finding of more extensive connectivity changes than magnitude changes would uncover another type of activation that has been previously overlooked in studies using univariate analyses of canonical functions representing the time course of the task. During brain activation, we hypothesize that extensive regions associated with carrying out calculations related to the task may show correlation changes but may not show a magnitude change that is reflected as a correlation with the expected canonical reference function typically used in SPM type analyses. {P. A. Bandettini, J. Gonzalez-Castillo, D. A. Handwerker}

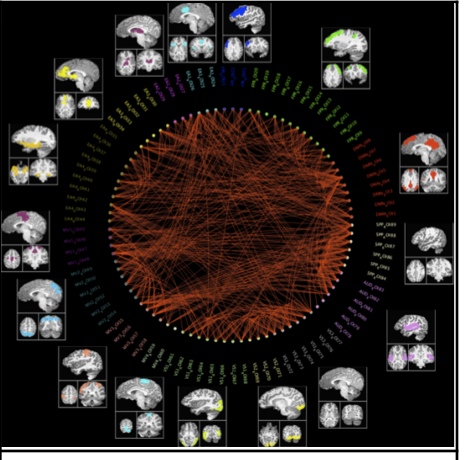


Figure 8: 100 run (9 hours of averaging for a single subject) data of a simple visual attention task showing the consistent connectivity changes across nearly all parcels in the brain.

1C-5. Resting state Frequency Signatures across Cortical Regions

Earlier work from SFIM showed that the correlation between different brain regions changes periodically over time[11]. One possible explanation for this observation is that fMRI time series have small, but consistently distinct frequency profiles. These regional frequency differences are usually hidden under much larger, common signal fluctuations. By calculating sliding window correlations over time, subtle differences are perhaps amplified as beat frequencies. For example, few people can distinguish two sounds that are 1Hz apart, but, if the tones are played together, a 1sec cycling of the signal volume is easily heard. In this study, we examined the power spectra (the strength of the time series fluctuations at different frequencies) of network-based regions of interest to see if these types of frequency variations are occurring between regions. The ability to characterize different time series in this manner would suggest that fMRI can probe subtle temporal dynamics that are typically examined using electrophysiological measures.

In this study, we examine if we can more directly identify these relative frequency differences. Data were collected as part of another study from our group [10] from 11 healthy adults as they were told to relax with their eyes closed for 60 minutes ($\text{TR}=1\text{s}$). Gray matter ROIs were made based on the 10 ICA-based networks defined in Smith et al.[25]. Our data didn't include a sufficient number of cerebellar voxels and the left and right frontoparietal networks were merged. The brain slices in Figure 9A show the 8 defined ROIs. For each ROI, an average power spectrum was calculated for each subject. The average and standard deviation of two ROI spectra

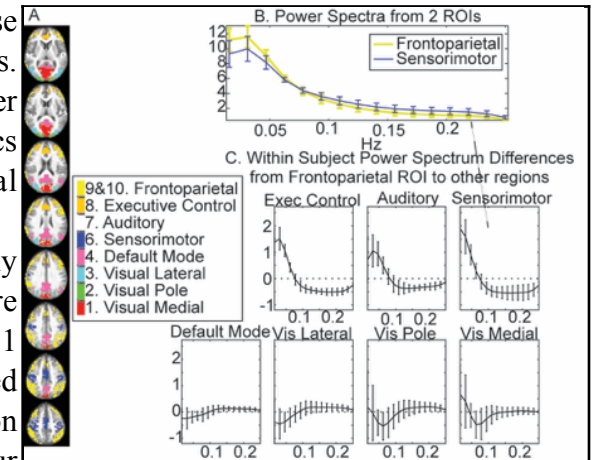


Figure 9: **A)** ROI's used to create time series power-spectra. **B)** Two power spectra from Regions 9&10 and Region 6. **C)** Difference spectra between the power spectra corresponding to the Frontoparietal region and all other regions. The arrow is pointing from the two spectra subtracted to create the spectrum to where the arrow is pointing.

across subjects are shown in Figure 9B. We then subtracted the spectra within each subject for each pair of ROIs. Figure 9C shows the power spectrum differences from the frontoparietal ROI to all other ROIs. There are consistent and distinct frequency differences across subjects for different pairs of network ROIs. These results suggest that these power differences between pairs of brain networks are hidden due to variation across individuals, but visible when comparing power spectral differences within individuals. *{P.A. Bandettini, J. Gonzalez-Castillo, D.A. Handwerker, C. Chang}*

Theme 2: Pushing the Limits of Hemodynamic Stability, Sensitivity and Specificity

2A. Introduction: *What more can we extract from hemodynamics?*

The second scientific focus of SFIM is on extracting as much information as possible from either resting-state or task-activated fMRI signal changes. In these past four years, we have advanced our initial findings on massively averaged fMRI data and have repeated the experiment at 7T on slightly modified tasks that include those that do not involve a motor response. With these experiments we demonstrated a “cognitive-load” dependence of these additional areas of activation and also categorized the extensive changes as transient, positive, or negative changes. Our findings include a confirmation of the previously hypothesized “task set change” region in the Insula. Analyses of these results also suggested with the experimental tasks, and likely most tasks, a majority of the brain shows negative signal changes. Using this data set we have also been able to characterize more fully different sources of noise as across session, across run, and within run. In this theme, we further demonstrate the effectiveness of multi-echo EPI for separating BOLD effects from non-BOLD effects in a time series. Specifically, in the past work section we report on our results for decreasing slow drift in long time series - allowing for the differentiation of non-typical long duration activations that are sensitive to time series drift.

With regard to ongoing work within this second theme, we are happy to have had Dr. Laurentius Huber recently join us as a post-doc. He brought with him several pulse sequences optimized for high resolution anatomic and functional imaging at 7T. In the context of this theme, we have used high resolution Vascular Space Occupancy (VASO) - sensitive to venous blood volume changes - to map activation related layer dependent activity in sensory and motor cortex during a finger tapping / movement-without-tapping task. We have also used this sequence to help determine the layer specificity of predominant resting state fluctuations across the cortical ribbon throughout the brain. These initial results are extremely exciting as they suggest that the exquisite capillary specificity of VASO gives unprecedented ability to map layer-specific activation and fluctuations. This ability, we hypothesize, will lead to directional input inferences based on layer input location, and therefore will move fMRI into the realm of teasing out directional cortical circuitry.

Lastly, we are working on methods for improving naturalistic paradigms that involve movie viewing. We demonstrate that the use of multi-echo EPI provides a significant boost in signal to noise for cross time series correlation analysis. Our ultimate goal is to develop a naturalistic paradigm to be used for comparison across normal and patient populations and to draw out individual differences in specific responses to aspects of the stimuli. Here we found that a multi-echo EPI sequence increases cross-run correlation sensitivity. Because of the transient nature of naturalistic paradigms, time series averaging may not be as viable as an option, therefore reinforcing a critical need for multi-echo EPI based denoising as it can improve time series stability.

2B. Past Studies

2B-1. Whole brain activation at 7T

In a previous study[12], we showed that when BOLD time series data are massively averaged, the majority of the brain shows statistically significant hemodynamic responses time-locked with the experimental paradigm. Such a finding questions localizationist views of brain function as well as the precise meaning of a spatial null-hypothesis in brain mapping.

The presence of distributed time-locked hemodynamic responses is not sufficient to make the claim that the entire brain is “activated” by these tasks as many of these waveforms could represent a “disengagement” of cortical regions in association with a task. To address this and other open questions, we carried out a follow up experiment on our 7T system [26].

First, the relationship between activation extent and task demands was investigated by varying cognitive load across participants. One subject performed a letter/number discrimination task superimposed on a full field-of-view (FOV) flickering checkerboard (same as in [12]); a second subject simply fixated on the center of a full FOV flickering checkerboard; and a third subject only received visual stimulation (i.e., flickering checkerboard) in the left hemifield of the FOV while fixating. Second, the tissue specificity of responses was probed by scanning at higher resolution afforded by the 7T. Finally, the spatial distribution of 3 primary response types—namely positively sustained (pSUS), negatively sustained (nSUS), and transient—was evaluated using a newly defined voxel-wise wave-shape index that permits separation of responses based on their temporal signature. About 86% of gray matter (GM) became significantly active when all data entered the analysis for the most complex task, as indicated in Figure 10. Activation extent scaled with task load and largely followed the GM contour. The most common response type was nSUS BOLD, irrespective of the

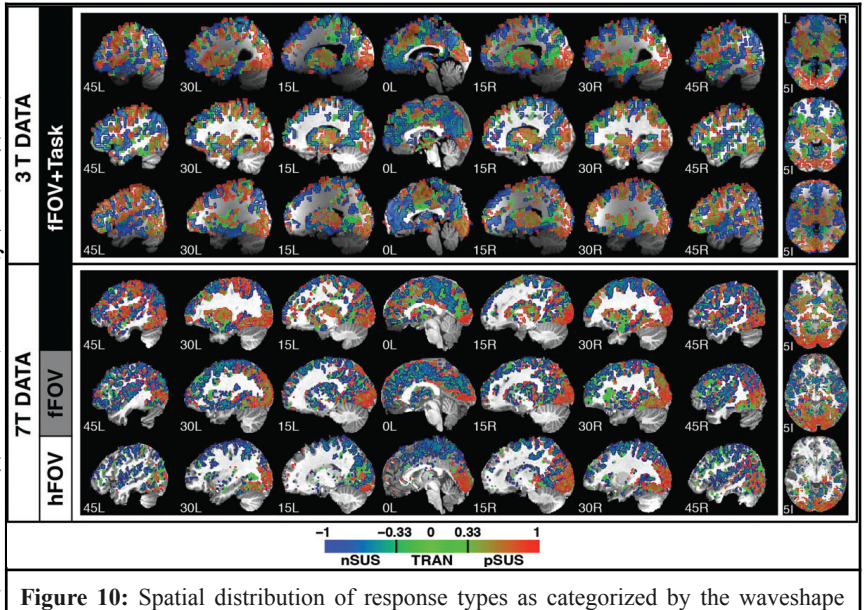


Figure 10: Spatial distribution of response types as categorized by the waveshape index (w) in a set of sagittal and axial slices for all 6 participants. A gradient scale was used to color each voxel according to its w index. Additionally, contours were overlaid in the map to depict the classification of voxels in 3 main primary response types: red=positively sustained responses ($0.33 < w < 1$); green=transient responses ($-0.33 < w < 0.33$); and blue=negatively sustained responses ($-1 < w < -0.33$).

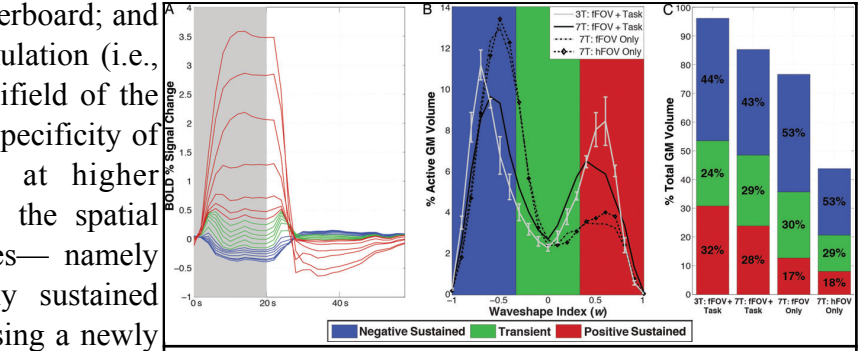


Figure 11: (A) Relative size of mean responses, as categorized by w into 20 bins, for active GM voxels in the 7T fFOV + Task subject. Positively sustained, transient, and negatively sustained responses are colored in red, green, and blue, respectively. (B) Histograms of w as a percentage of active GM for each subject (average of 3T subjects shown with standard error bars), showing the relative abundance of each response type. (C) Bar graph showing contributions of each response type relative to total GM volume for all 7T and the average of the 3T subjects. The percentage of GM activation that each response type is responsible for in each subject is overlaid in black.

task, as shown in Figure 11.

These results suggest that widespread activity associated with extremely large single-subject fMRI datasets can provide valuable information about the functional organization of the brain that goes undetected in smaller sample sizes. They also constitute additional evidence in support of a biological significance for widespread BOLD signal changes in larger-than-usual fMRI datasets. Lastly, while much of the brain does show de-activation, evidence from 1B-1 suggests that the larger spatial extent of BOLD signal changes may help discriminate specific tasks, thus containing information about the task as opposed to a more general “deactivation” response. This work has been reported in Cerebral Cortex [26]. {P. A. Bandettini, R. W. Cox, J. Gonzalez-Castillo, D. A. Handwerker, C. W. Hoy, S. J. Inati, V. Roopchansingh, Z. S. Saad}

2B-2. Multi-Echo EPI for slow change assessment

Multi-echo acquisition is more frequently used in quantitative T2* measurements than in fMRI. In the context of fMRI, the acquired echoes can be combined to improve the overall image SNR and recover signal dropout. The recently developed multi-echo (ME-ICA) denoising method[19] uses TE-dependence throughout the analysis pipeline to separate time series into BOLD and non-BOLD signal in an automatic, data driven way that is based on the principle that BOLD contrast is simply a change in T2*, while all other changes, as measured by the multi-echo acquisition (TE=0 intercept - suggesting T1 or proton density change), are non-BOLD and do not show TE dependence. ME-ICA differs from other automated ICA component selection methods in that no restrictions are placed on the time–frequency or anatomical localization characteristics of the components in the selection process. Therefore, it has the potential to separate artifactual, hardware-related drifts, which would fall into the non-BOLD subspace, from hemodynamic signal changes that are likely of neuronal relevance. Importantly, this enables study of low-frequency BOLD components that would ordinarily be discarded in the band-pass filtering step that is applied during preprocessing.

In this study, we used a visual task with slowly changing contrast over 5 min as an example of a slow BOLD change. We compare conventional acquisition and processing to ME-ICA denoising[19]. We demonstrate the ability to separate a slowly changing or long duration constant task response from baseline drifts using ME-ICA denoising in a case where the task is undetectable in conventionally preprocessed data. Figure 12 shows a comparison between a weighted average “optimally combined”(OC) multi-echo data set, de-trended OC data, and multi-echo denoised data, clearly demonstrating the ability for ME-ICA to even differentiate a sigmoidal visual stimulation contrast evolution over 300 seconds vs a linear contrast evolution (bottom right plot). This work has been published in NeuroImage [27]. {P. A. Bandettini, J. W. Evans, S. G. Horowitz, P. Kundu}

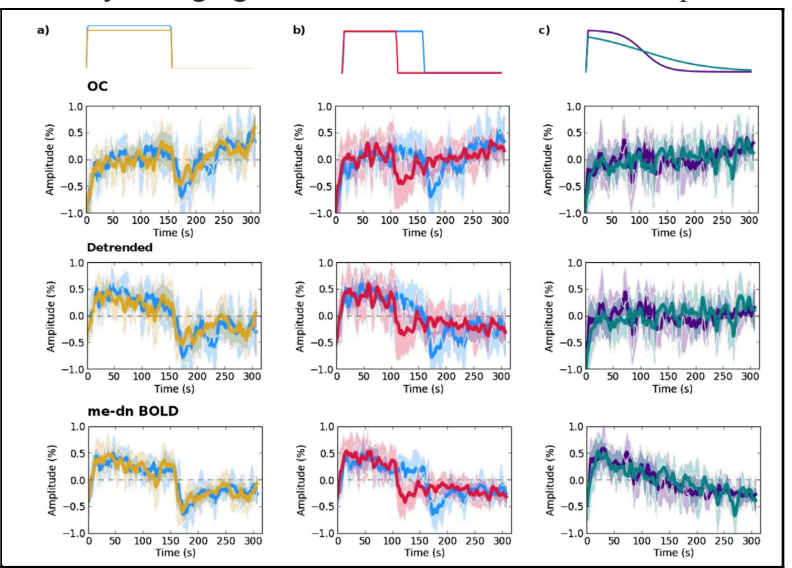


Figure 12. Comparison between optimally combined (OC), detrended OC, and multi-echo denoised (me-dn) time series for 300 second stimulation runs, clearly showing the ability of me-dn to stabilize even a long baseline.

2C. Current Studies

2C-1. Layer specific mapping in sensory and motor cortex at 7T using VASO

The cortex consists of up to six cortical layers. Based on the different anatomically defined input-output characteristics across cortical layers, individual brain areas are expected to show different layer-dependent activity profiles according to their feed-forward/feed-back input. High-field high-resolution fMRI on a layer-dependent level might be able to elucidate afferent and efferent functional connectivity in healthy human volunteers using task activation or even resting state fMRI signal.

Here, we report on an fMRI acquisition and analysis method that we are developing to measure layer-dependent activation and fluctuations. To account for limited signal-to-noise-ratio at sub-millimeter resolutions, acquisition and reconstruction strategies were optimized on a subject specific level, including custom designed RF-coil combination schemes, field of view geometry, application of FLASH-GRAPPA, and 7T field strength. In order to minimize effects of locally non-specific large draining veins in conventional GE-BOLD fMRI, we sought to map layer-dependent activity using measures of cerebral blood volume (CBV) with VASO[28]. VASO is understood to be sensitive to blood volume changes. Evidence suggests that activation-induced blood volume changes are localized to the microvasculature whereas BOLD contrast is sensitive to blood oxygenation changes in all vasculature.

We used the above approach for both a task (finger tapping vs finger movement without tapping) and for resting state fluctuation assessment. We found significant finger-tapping induced activity on a layer-dependent scale. The laminar distribution of task-induced activity and resting-state correlation results are observed to be specific to the unique input-characteristics for the corresponding tasks and resting-state seed regions.

Figure 13A shows that fMRI signal in upper layers of primary motor cortex (M1) have highest correlation values with resting-state fluctuations in primary sensory cortex, in line with the understanding that M1 receives its input from primary sensory cortex (S1) in upper cortical layers as opposed to the deeper layers. This result was further validated by comparing task-induced activity in M1 for finger-tapping involving finger tip touching compared to finger-movement without touch. The non-touching tasks differ in reduced exteroception in S1 and correspondingly reduced S1-input into M1. Figure 13B shows the corresponding layer-profiles for finger-tapping activity in M1 with and without touching. These results confirm the resting state results, namely that input from S1 into M1 is localized in upper cortical layers.

We have taken our resting

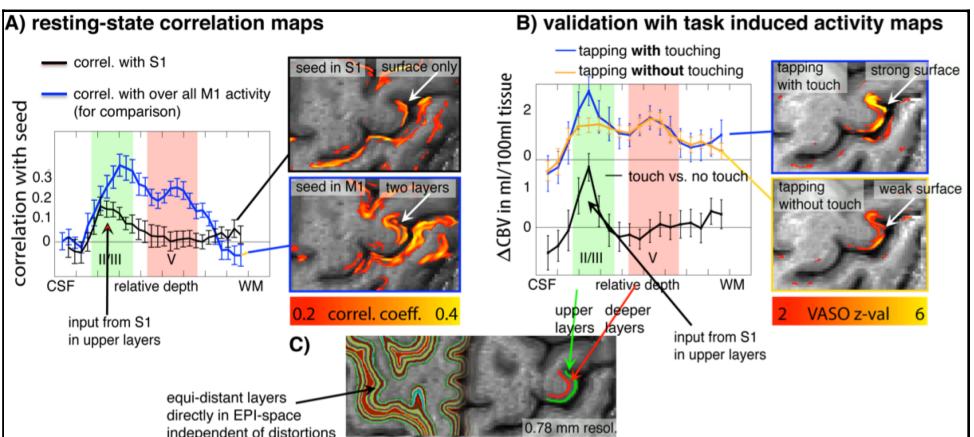


Figure 13: A) Layer specificity of resting state fluctuations. M1 appears to have most resting-state fluctuation energy in the upper as well as the lower layers(blue line), however only the upper layers show a strong correlation with a seed in S1 (black line), suggesting input from S1 occurring here. B) Validation of the resting state results based on comparing task-induced activity with differing sensory activity: tapping with (blue line) and without (yellow line) touching. This modulation clearly alters the activity in layer II and III of motor cortex - again suggesting that this is layer that receives touch-specific sensory input. C) Illustration of cortical layering and position of upper and lower layers used in Figures A and B.

state analysis further, classifying the fluctuations in cortical ribbon as being either upper layer dominated, upper and lower layer dominated, and middle layer dominated. A single slice showing this preliminary classification of fluctuation location appears to give clear results showing a differential classification between frontal, motor and parietal regions. This map is shown in Figure 14.

We conclude that the application of the proposed resting-state fMRI protocol can help to investigate underlying feed-back/feedforward characteristics of resting-state networks and their inter-laminar connectivity[29]. {P. A. Bandettini, J. Gonzalez-Castillo, D. Handwerker, **L. Huber**, D. Jangraw, S. Marret, B. A. Poser}

2C-2. Multi-echo EPI and Improvements on Massive Trial Repetition

ME-ICA has been demonstrated as a way to empirically identify and remove non-BOLD signal from fMRI time series to improve the contrast to noise ratio. We examined how ME-ICA based fMRI could be used to improve activation extent. A goal of this study was to first determine if ME-ICA can achieve the previously found extensive activation - from single-echo time series - with less data. For each analysis, we compared single-echo fMRI (middle echo of the multi-echo acquisition), the “Optimally Combined” weighted average of the 3 echoes, and the “de-noised” result of the ME-ICA analysis.

The task was to identify numbers or letters in a flashing checkerboard. The timing was a 20 sec on and 20 sec off blocked design. The task and timing was identical to that described in Gonzalez-Castillo et al. [12]

As Figure 15 shows, multi-echo EPI substantially improved sensitivity - as measured by the fraction of voxels passing statistical threshold for a given number of averages. The largest differences were observed between 10 and 40 averages. With Volunteer 1, the same results as with 100 runs could be obtained with about half the number of averages. Also, there was an over 30% activation extent increase when fewer than 10 runs were used. Volunteer 1 showed an additional large increase of ME-ICA denoised data over Optimally Combined. Further work needs to be performed to understand the remaining sources of noise in ME-ICA so that the results are consistently better than Optimally Combined as well. {P.A. Bandettini, L. Buchanan, J. Gonzalez-Castillo, B.E. Gutierrez, **D.A. Handwerker**, D.C. Jangraw, V. Roopchansingh}

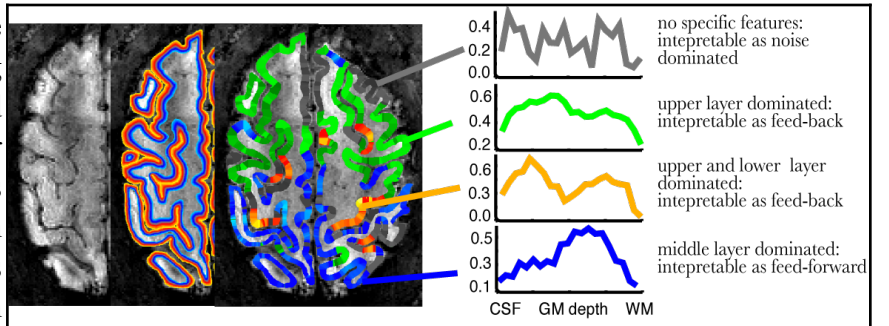


Figure 14. Spatial features: M1 is dominated from fluctuations in upper and lower cortical layers (orange). S1 is dominated from fluctuations in middle cortical layers. Frontal cortex is dominated by upper layer fluctuations. Parietal regions are dominated, as is S1, by middle layer fluctuations. This layer dependence may allow maps of relative feedback vs feed-forward circuits to be disentangled.

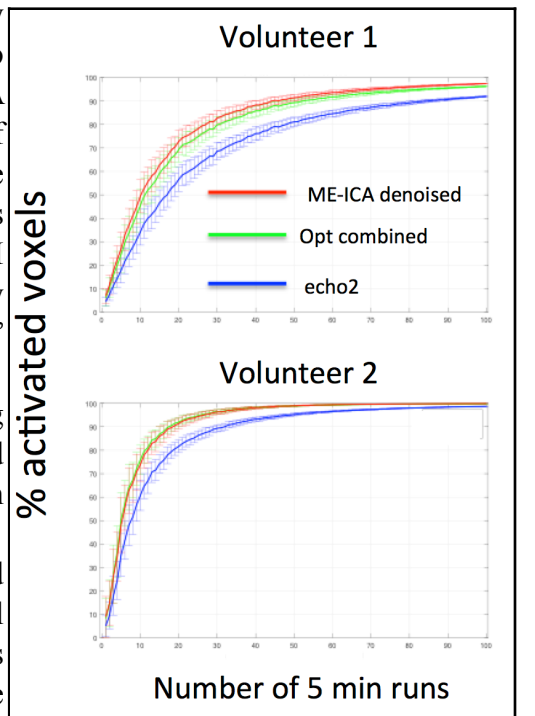


Figure 15. Percent activated voxels as a function of the number of 5 min runs.

2C-3. Cross run correlation improvements with multi-echo EPI

As fMRI researchers increasingly tackle naturalistic, complex experimental paradigms, response *reliability* is often used in place of response *amplitude or magnitude* as a metric of each voxel's responsiveness to a stimulus. To determine voxel response reliability, a voxel's response from one run is used as a model for the same voxel's response in the other runs, a process that is repeated for each possible pairing of runs. Voxels with "reliable" responses are those that consistently show large positive correlations across pairings[30]. This approach, often called intra-subject correlation analysis, is especially useful in cases where the stimulus cannot be used to create a simple canonical reference function - as in the case of free viewing of a naturalistic movie. Such studies have revealed many areas of consistent activation in both across-subject and within-subject groupings, inspiring more researchers to adopt the approach. But the relatively unconstrained nature of these paradigms translates to a low contrast-to-noise ratio, so response reliability measures have much to gain from de-noising techniques.

To this end, we applied ME-ICA[18], to data from the free viewing of a naturalistic movie. In the current study, two subjects watched a 7-minute cartoon movie 16 and 17 times respectively across multiple days. We then analyzed the intra-subject correlations of voxels across runs. The response reliability was assessed in this way both with and without ME-ICA de-noising.

The ME-ICA results demonstrate that the movie evokes reliable brain-wide activation that is much more extensive than standard data collection and processing methods might suggest. When ME-ICA was used instead of standard single-echo processing, the number of voxels showing significant activation (FDR corrected $q<0.05$) increased from 21% to 47% in subject 1 and from 22% to 34% in Subject 2. This is shown in Figure 16. The voxels whose response reliability was revealed by ME-ICA but not by single-echo processing are significantly more likely to be in gray matter than in-brain voxels chosen at random (one-tailed binomial test, $p<1e-15$), suggesting that they are driven by neural activity. Preliminary analyses indicate that some of these areas are driven by high-level properties of the movie such as the presence of faces and the whole-body motion of characters. With this sensitivity boost, future studies using intra-SC will be more likely to find more subtle as well as more reliable responses to naturalistic stimuli. This could lead to diagnostic tools based on targeted movies that capture the scenarios where symptoms are typically observed. {P. A. Bandettini, J. Gonzalez-Castillo, B. Gutierrez, D. A. Handwerker, D. C. Jangraw}

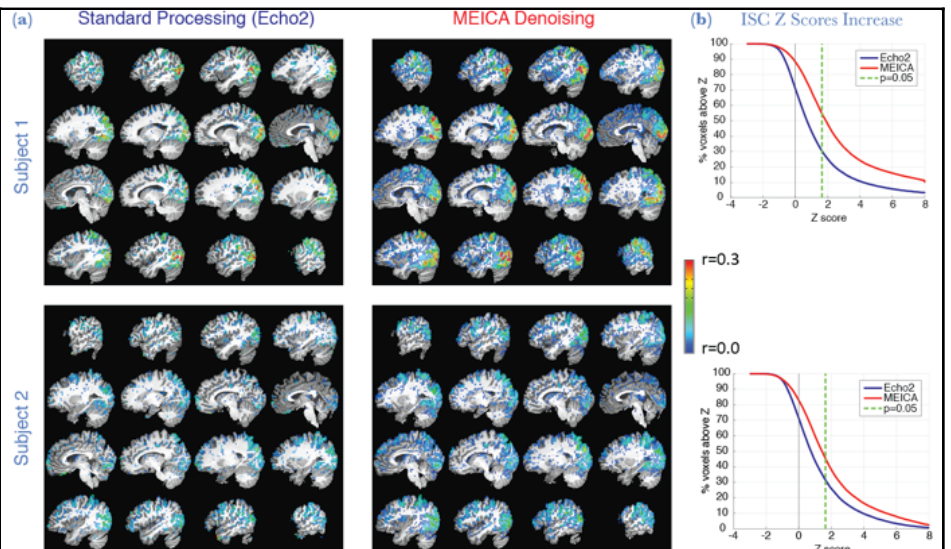


Figure 16: A) Average correlation coefficient r across intra-SC pairings, thresholded at FDR-corrected $q<0.05$ for Subject 1 and 2, using Echo 2 (left) or ME-ICA denoised (right) time series as input. B) Reverse cumulative histogram of voxel-by-voxel Z scores across the whole brain for Subject 1 (top) and 2 (bottom).

Theme 3: Novel Contrasts and Interventions

3A. Introduction: *Expanding the utility of fMRI and MRI*

The third SFIM research theme is a step outside the work on fMRI connectivity, dynamics, and resolution. The focus here is on pushing the limits of what can be done with MRI in general and how interventions other than brain activation may influence MRI and fMRI signal. Our primary completed project has been a study that characterizes anatomic changes in hippocampus with an exercise intervention over the course of several weeks. The finding was that that anterior hippocampus increases in size[3, 6]. In this work we apply several different contrast weightings to determine what is actually changing with this intervention.

Our ongoing work within this third theme involves better understanding of BOLD signal changes that rapidly occur during the Valsalva maneuver - as this maneuver may turn out to be a relatively easy means by which global hemodynamic changes are induced - allowing for easily calibrated fMRI. For calibrated fMRI, a stress such as hypercapnia is used to cause a global flow change without an increase in cerebral metabolic rate. Such a map corresponding to a whole-brain flow increase reflects, essentially, the BOLD weighting function for all voxels. Obtaining this with more ease would be desirable. The Valsalva maneuver produces similar maps to those created with hypercapnia; however, we don't fully understand the underlying vascular events leading to our observations. In this study we use VASO - a method for observing blood volume changes - during the Valsalva maneuver.

In a followup to the above study on changes in hippocampal volume with exercise, we have determined, using a susceptibility-weighted anatomic imaging approach, that iron deposition in the basal ganglia increases with fitness. Following up on our layer dependent resting state and activation study, we have compared the performance of 3D-EPI-VASO with SMS-VASO and found that each is superior in a specific context. Incidentally, using a high resolution and high speed T1 quantification sequence, we found a localized T1 increase in gray matter associated with brain activation. We also detected a corresponding 5% swelling in gray matter volume. We are currently investigating the source of the rapid gray matter volume change.

3B. Past Studies

3B-1. Anterior Hippocampal Volume Increase with Aerobic Exercise

The hippocampus has been shown to demonstrate a remarkable degree of plasticity in response to a variety of tasks and experiences. For example, the size of the human hippocampus has been shown to increase in response to aerobic exercise. However, it is currently unknown what specific mechanisms underlie these changes. This study is a collaboration with Heidi Johansen-Berg's group in Oxford, carried out by Adam Thomas as part of his Ph.D. thesis work. Animal and human studies provide a number of candidate mechanisms for exercise-driven or experience-dependent change in brain structure. For example, it has been shown that aerobic exercise increases the rate of neurogenesis in the dentate gyrus region of the rodent hippocampus and increases CBV in the same region in humans. Environmental enrichment, a less specific manipulation, has been shown to increase myelination of corpus callosum fibers. In rats, some effort has been made to relate the morphometric measurements commonly used in neuroimaging to underlying changes in the neural tissue elicited by other behavioral training paradigms, but little is known about what drives these changes in humans.

Our goals in designing this experiment were threefold: First, to explore hippocampal volume change with increased aerobic exercise in a younger population and on a shorter time scale than previously shown; Second, to determine if this volume change is maintained in the absence of continued aerobic exercise; And third, to attempt to use multi-modal MRI to explore what might be driving the hippocampal volume change. Based on prior histological studies, we specifically chose to explore potential changes in both vasculature and myelination.

Here we scanned sedentary, young to middle-aged human adults before and after a six-week aerobic exercise intervention using nine different neuroimaging measures of brain structure, vasculature, and diffusion. Surprisingly, we found no evidence of a vascular change as has been previously reported. Rather, the pattern of changes is better explained by an increase in myelination as shown in Figure 17. Finally, we showed that hippocampal volume increase is temporary, returning to baseline after an additional six weeks without aerobic exercise. This is the first demonstration of a change in hippocampal volume in early to middle adulthood suggesting that hippocampal volume is modulated by aerobic exercise throughout the lifespan rather than only in the presence of age related atrophy. It is also the first demonstration of hippocampal volume change over a period of only six weeks, suggesting that gross morphometric hippocampal plasticity occurs faster than previously thought. This study was recently published in NeuroImage[6]. {P. A. Bandettini, H. Dawes, A. Dennis, S. Foxley, L. Matthews, M. Morris, M. Jenkinson, H. Johansen-Berg, S. H. Kolind, T. Nichols, N. B. Rawlings, C. J. Stagg, A. G. Thomas}

3C. Current Studies

3C-1. Iron deposition in basal ganglia increases with fitness.

It has been well established that the amount of iron in several basal ganglia structures increases asymptotically with age, and is a feature of neurodegenerative disease. The significance of this iron accumulation is not well understood however. The purpose of this study was to understand the relationship between age, fitness, cognition and iron deposition in the brain.

Fifty-six participants (33 women, mean age 32.1, S.D. 10.8) underwent fitness and cognitive assessment as well as a 3T MRI scan. The fitness test was a continuous, incremental test conducted on a cycle ergometer. Cerebral Blood Volume (CBV) was measured using two MPRAGE scans collected before and after contrast agent injection (Dotarem, 0.1ml/kg). Susceptibility weighted images (SWI) were collected using a standard multi-echo SWI sequence distributed by Siemens

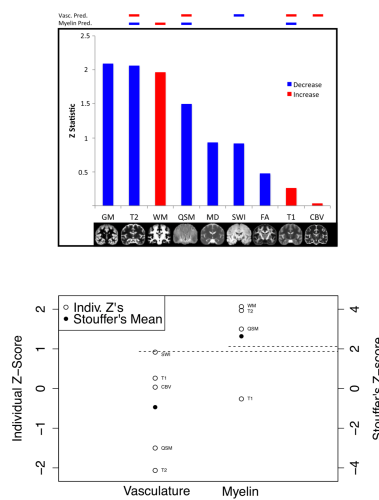


Figure 17. Top: Z-scores of change in each measure from before to after exercise in anterior hippocampus. Decreases shown in blue and increases in red. Bottom: Plot of Z-scores from individual tests (open circles) predicted in the case of an increase of vasculature vs. a predicted increase in myelination (scale for both is shown on left Y-axis). This Z-score is significant for the myelin test ($Z = 2.64$) but not for the vasculature test ($Z = -1.05$). GM = gray matter, WM = white matter, QSM = quantitative susceptibility map, MD = mean diffusivity, SWI = susceptibility-weighted image, FA = fractional anisotropy, CBV = cerebral blood volume.

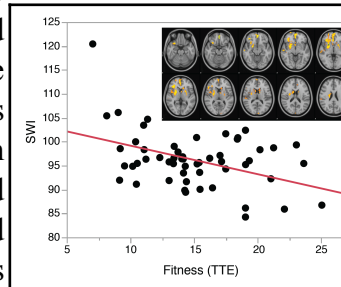


Figure 18. Two clusters in the right putamen and medial frontal cortex show regions of positive correlation between fitness and susceptibility. Yellow shows sub-threshold regions of positive correlation. Bottom: Scatter plot shows susceptibility values for the green regions vs. TTE to visualize the distribution of values.

with 1.3 mm isotropic voxels, TE = 6.72 ms & 24.60 ms, TR = 30 ms, matrix size = 192 x 192, and GRAPPA factor = 2.

We found no relationship between any cognitive measure and the age-related accumulation of iron in the basal ganglia during young to middle adulthood. However, we do show that susceptibility correlates with fitness. Figure 18 shows two clusters in the right putamen and medial frontal cortex that show linear relationship between SWI signal (inversely proportional to the susceptibility source concentration) and fitness, suggesting iron deposition may be a by-product of cardiovascular activity. {P. A. Bandettini, H. Dawes, A. Dennis, H. Johansen-Berg, N. B. Rawlings, C. J. Stagg, A. G. Thomas}

3C-2. Exploring Valsalva-induced changes using VASO

The Valsalva Maneuver involves an increase in intrathoracic pressure during a breath hold that alters blood pressure and heart rate. We recently published work that shows, for a constant breath hold duration, the fMRI BOLD-weighted response scales with chest pressure magnitude. Both the undershoot during the breath hold and the signal peak after the hold ends increases with increasing pressure[4]. This parametric modulation of cerebrovascular reactivity by pressure has the potential to be used as a relatively simple cerebrovascular reactivity probe, however the mechanisms underlying the fMRI signal changes aren't fully understood. We are continuing this work using Vascular Space Occupancy (VASO) to measure BOLD-weighted and blood volume-weighted changes during Valsalva challenges to determine to what degree and at what phase of the Valsalva maneuver, blood volume changes contribute. Hypothesized mechanisms for the rapid decrease in signal is either an increase in blood volume, a decrease in flow, or a decrease in the presence of CSF in the same regions that have highest blood volume. Subsequent increases in signal may also be explained by the same variables reversing in sign.

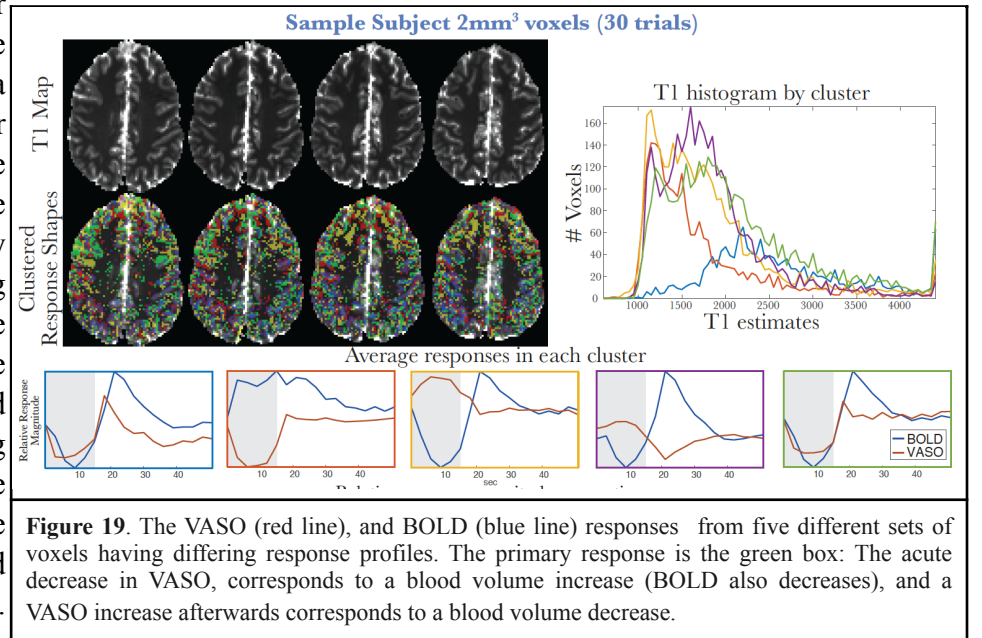


Figure 19. The VASO (red line), and BOLD (blue line) responses from five different sets of voxels having differing response profiles. The primary response is the green box: The acute decrease in VASO, corresponds to a blood volume increase (BOLD also decreases), and a VASO increase afterwards corresponds to a blood volume decrease.

We collected 7T data using variants of the VASO sequence described in Huber et al. [31]. Each run includes multiple trials of paced breathing followed by a Valsalva Maneuver or breath hold without chest pressure feedback. The Figure 19 shows that breath hold causes a whole-brain BOLD-weighted response. As shown previously, the BOLD signal has two phases - below baseline with the onset of the Valsalva Maneuver and above baseline during the recovery period. The VASO-weighted response is also whole-brain, but the signal magnitude changes have a distinct spatial profile. Continuing work will compare the temporal and spatial profiles of these responses to better understanding what cerebrovascular mechanisms underlie the response to the Valsalva Maneuver. (P.A. Bandettini, J. Gonzalez-Castillo, B.E. Gutierrez, D.A. Handwerker, L. Huber, P. Panwar, P. Wu)

3C-3. Blood volume fMRI with 3D-EPI-VASO: Any benefits over SMS-VASO?

Quantitative cerebral blood volume (CBV) fMRI has the potential to overcome several limitations of BOLD fMRI. In particular, it offers superior localization specificity down to the level of cortical layers and its quantitative nature helps to better understand and ‘calibrate’ the conventional BOLD response. Non-invasive CBV-fMRI with VASO (Vascular Space Occupancy), however, is inherently a single-slice approach and limited with respect to its imaging coverage. This limitation can be overcome with recently developed advanced readout strategies such as simultaneous multi-slice (SMS) EPI or 3D-EPI. With these imaging strategies, reductions in volume acquisition times can be achieved by parallel acceleration along the secondary phase encoding direction and minimal g-factor penalty using controlled aliasing with blipped CAIPIRINHA.

In this study we sought to overcome coverage limitations that are involved with VASO data collection by combining it with the advanced readout methods of 3D-EPI and SMS-EPI and comparing them across a wide range of resolutions at 7T. Results in Figure 20A show that the temporal stability and the corresponding sensitivity to detect finger tapping activity is higher for 3D-EPI-VASO compared to SMS-VASO in the thermal noise dominated regime of sub-millimeter resolutions. In the physiological noise dominated regime at lower resolutions, however, SMS-VASO shows better performance compared to 3D-EPI-VASO. So, in the presence of a temporal signal to noise higher than about 30, it is recommended to use 2D EPI or SMS, but when below 30, it is recommended to use 3D EPI for VASO.

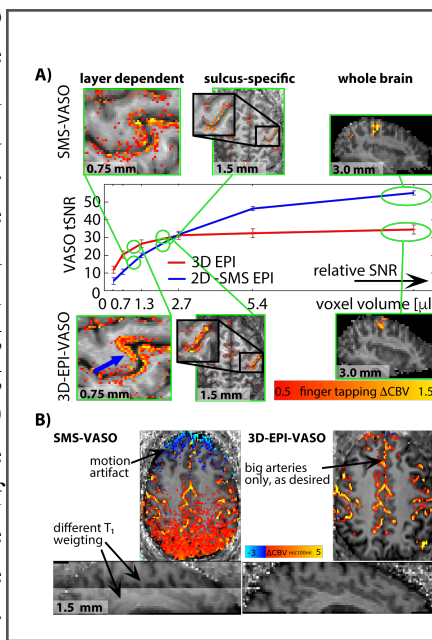


Figure 20. **A)** Activation maps of CBV change [$\text{ml}/100\text{ml}$ tissue] for right hand finger tapping across a wide range of resolutions, acquired with 3D-EPI-VASO. Note the localized specificity of CBV changes to layer-dependent activity (blue arrow) and to individual GM bands in the central sulcus (red arrow). **B)** SMS-VASO and 3D-VASO results for a breath holding experiment with task-induced head motion. Note that the different T₁-weighting in different slices of SMS-VASO can result in severe motion artifacts.

Figure 20B shows results for a breath hold experiment with task induced head tilting. It can be seen that even with an inferior sensitivity, at low resolutions, 3D-EPI-VASO can be more practical than SMS-VASO, as it can better be used to account for motion artifacts. We conclude that because of its superior sensitivity at ultra high resolution, and its reduced sensitivity to head motion 3D-EPI VASO may play an important role in VASO-fMRI. {P.A. Bandettini, D. Handwerker; L. Huber, D. Ivanov, S. Marret, P. Panwar, B. A. Poser, K. Uludağ}

3C-4. Fast Dynamic Measurement of Functional T₁ and Grey Matter Thickness

The acquisition of multi-shot high-resolution anatomical T₁-weighted brain images plays a key role in the daily routine of neuroscience. Specifically it is widely used to image anatomical features, e.g. with respect to pathological anomalies, anatomical changes in plasticity-studies, and it is used as an anatomical reference in fMRI studies. In these application however, quantitative T₁-imaging is limited by its relatively long acquisition times of several minutes, and its application in fMRI-studies is limited by having different distortions compared to EPI-based functional data.

Recent developments of advanced through-plane acceleration involving multi-band excitation with controlled CAIPI-aliasing, and the advent of advanced in-plane acceleration with FLEET or FLASH GRAPPA reference lines boosted the imaging efficiency of EPI-based acquisition methods to achieve high-resolution whole brain coverage within a few seconds, with comparable signal quality as multi-shot ‘anatomical’ MRI.

Here we test the applicability of state-of-the-art SMS-FLEET-EPI in combination with inversion-recovery preparation to obtain high-resolution quantitative T_1 -maps within 3 seconds with distortion-matched geometry compared to functional scans.

Figure 21A depicts the image quality of a quantitative T_1 -map acquired within 9 sec in a representative health volunteer. Figure 21B and C show the application of the new T_1 -mapping scheme as an anatomical reference for EPI-based functional results. Figure 21B depicts a representative potential artifact of using unmatched distortions as a reference (green arrows), and how it can be avoided with the new distortion-matched EPI-based T_1 -map. The distortion matched T_1 -map can better delineate the cortical ribbon, even down to the level of cortical layers. Figure 21C shows an example, where unmatched distortions of the MP2RAGE-reference shift an M1/S1-activity blob more anterior; resulting in falsely insignificant activity in S1.

Figure 21D shows how the reduced acquisition duration of the EPI-based T_1 -mapping can be used in plasticity studies. The TR of 3 sec can help to track rapid changes of anatomical features, such as GM- T_1 , or cortical thickness on the fly, while they arise. When performing a finger-tapping task, the EPI-based T_1 -mapping can detect T_1 -increases up to 100 ms and GM-swelling up to 5%.

{P.A. Bandettini, D. Handwerker, L. Huber, D. Jangraw, S. Marrett, B. A. Poser, A. Thomas}

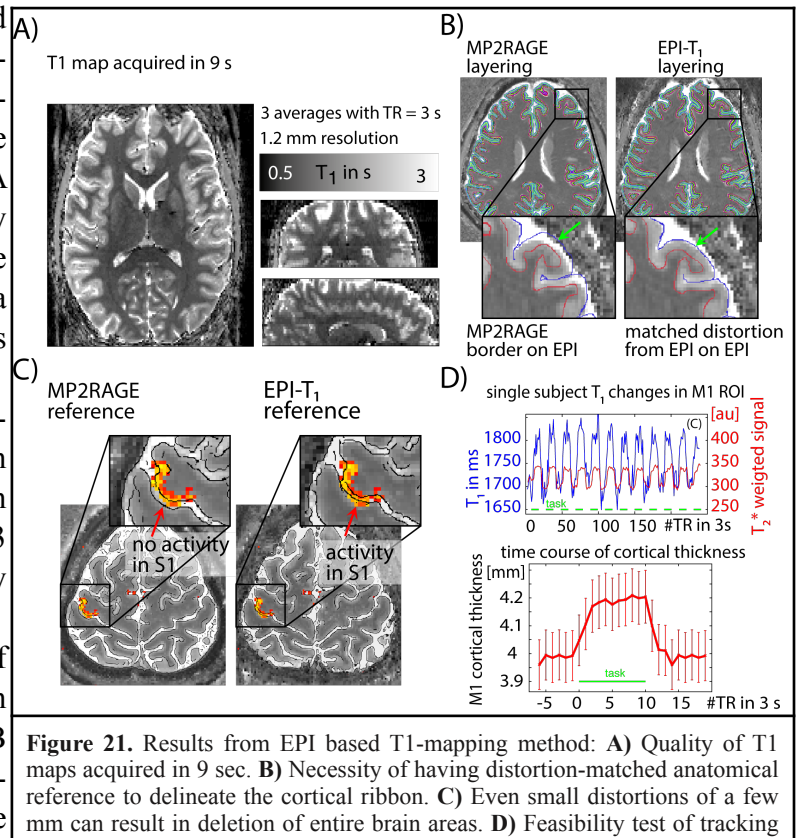


Figure 21. Results from EPI based T_1 -mapping method: **A)** Quality of T_1 maps acquired in 9 sec. **B)** Necessity of having distortion-matched anatomical reference to delineate the cortical ribbon. **C)** Even small distortions of a few mm can result in deletion of entire brain areas. **D)** Feasibility test of tracking anatomical “plasticity-changes” while they occur during a finger tapping task.

List of SFIM publications since last BSC report (papers featured in BSC report are in red)

1. D. A. Handwerker, V. Roopchansingh, P. A. Bandettini, Periodic changes in brain connectivity, NeuroImage 63, pp. 1712-1719 (2012).
2. Z. Yang, X.-N Zuo, P. Wang, Z. Li, S. M. LaConte, P. A. Bandettini, X. P. Hu, Generalized RAICAR: Discover homogeneous subject (sub)groups by reproducibility of their intrinsic connectivity networks, NeuroImage 63, pp. 403-414 (2012)
3. R. Kaplan, C. F. Doeller, G. R. Barnes, V. Litvak, E. Duzel, P. A. Bandettini, N. Burgess, Movement-related theta rhythm in humans: coordinating self-directed hippocampal learning. PloS Biology, 10, e1001267 (2012).
4. **A. G. Thomas, A. Dennis, P. A. Bandettini, H. Johansen-Berg**, The effects of aerobic activity on brain structure. Frontiers in Psychology, 3, pp. 1-9 (2012).
5. P. A. Bandettini, The BOLD plot thickens: sign- and layer-dependent hemodynamic changes with activation. Neuron 76, pp. 468-469 (2012)
6. J. Gonzalez-Castillo, K. N. Duthie, Z. S. Saad, C. Chu, P. A. Bandettini, W.-M. Luh, Effects of image contrast on functional MRI image registration. NeuroImage, 67, pp. 163-174 (2013).
7. W.-M. Luh, S. L. Talagala, T.-Q. Li, P. A. Bandettini, Pseudo-continuous arterial spin labeling at 7T for human brain: estimation and correction for off-resonance effects using a prescan, Magn. Reson. Med. 69, pp. 402-410 (2013).
8. M. Misaki, W.-M. Luh, P. A. Bandettini, Accurate decoding of sub-TR timing differences in stimulations of sub-voxel regions from multi-voxel response patterns. NeuroImage, 66, pp. 623-633 (2013).
9. M. Misaki, W.-M. Luh, P. A. Bandettini, The effect of spatial smoothing on fMRI decoding of columnar-level organization with linear support vector machine. Journal of Neuroscience Methods, 212, pp. 355-361 (2013).
10. **P. A. Bandettini, P. Kundu, J. Gonzalez-Castillo, M. Misaki, P. Guillod**, Characterizing and Utilizing fMRI Fluctuations, Patterns, and Dynamics, Progress in Biomedical Optics and Imaging – Proceedings of SPIE Vol 8672, doi: 10.1117/12.2012737 (2013).
11. K. Murphy, R. M. Birn, P. A. Bandettini, Resting state fMRI confounds and cleanup, NeuroImage, 80, pp. 349-359 (2013).
12. P. Kundu, N. D. Brenowitz, V. Voon, Y. Worbe, P. E. Vertes, S. J. Inati, Z. S. Saad, P. A. Bandettini, E. T. Bullmore, An Integrated Strategy for Improving Functional Connectivity Mapping Using Multi-Echo EPI, PNAS, 110, pp. 16187-16192 (2013).

13. R. M. Hutchison, T. Womelsdorf, E. A. Allen, P. A. Bandettini, V. D. Calhoun, M. Corbetta, S. D. Penna, J. H. Duyn, G. H. Glover, J. Gonzalez-Castillo, D. A. Handwerker, S. Keiholz, V. Kiviniemi, D. A. Leopold, F. de Pasquale, O. Sporns, M. Walter, C. Chang, Dynamic functional connectivity: promise issues, and interpretations. *NeuroImage*, 80, pp. 360-378 (2013).
14. M. Mur, M. Meys, J. Bodurka, R. Goebel, P. A. Bandettini, N. Kriegeskorte, Human object-similarity judgments reflect and transcend the primate-IT object representation. *Frontiers in Psychology*, 4, MAR (2013)
15. A. Devor, P. A. Bandettini, D. A. Boas, J. M. Bower, R. B. Buxton, L. B. Cohen, A. M. Dale, G. T. Einevoll, P. T. Fox, M. A. Franceschini, K. J. Friston, J. G. Fujimoto, M. A. Geyer, J. H. Greenberg, E. Halgren, M. S. Hamalainen, F. Helmchen, B. T. Hyman, A. Jasanoff, T. L. Jernigan, L. L. Judd, S.-G. Kim, D. Kleinfeld, N. J. Kopell, M. Kutas, K. K. Kwong, M. E. Larkum, E. H. Lo, P. J. Magistretti, J. B. Mandeville, E. Masliah, P. P. Mitra, W. C. Mobley, M. A. Moskowitz, A. Nimmerjahn, J. H. Reynolds, B. R. Rosen, B. M. Salzberg, C. B. Schaffer, G. A. Silva, P. T. C. So, N. C. Spitzer, R. B. Tootell, D. C. Van Essen, W. Vanduffel, S. A. Vinogradov, L. L. Wald, L. V. Wang, B. Weber, A. G. Yodh, The challenge of connecting the dots in the B.R.A.I.N., *Neuron*, 80, pp. 270-274, (2013).
16. H. J. Jo, S. J. Gotts, R. C. Reynolds, P. A. Bandettini, A. Martin, R. W. Cox, Z. S. Saad, Effective preprocessing procedures virtually eliminate distance-dependent motion artifacts in resting state fMRI. *Journal of Applied Mathematics*, 2013, Article # 935154 (2013).
17. L. Kenworthy, G. L. Wallace, R. Birn, S. C. Milleville, L. K. Case, P. A. Bandettini, A. Martin, Aberrant neural mediation of verbal fluency in autism spectrum disorders. *Brain Cogn.* 83, pp. 218-226 (2013).
18. Z. Yang, C. Chang, T. Xu, L. Jiang, D. Handwerker, F. X. Castellanos, M. Milham, P. Bandettini, X.-N. Zuo, Connectivity Trajectory across Lifespan Differentiates the Precuneus from the Default Network, *NeuroImage*, 89, pp. 45-56 (2014).
19. Z. Yang, P. Wu, P. A. Bandettini, X. Weng, The cerebellum engages in automation of verb-generation skill, *Journal of Integrated Neuroscience Volume 13*, pp. 1-17 (2014).
20. R. Kaplan, A. J. Horner, P. A. Bandettini, C. F. Doeller, N. Burgess, Human hippocampal processing of environmental novelty during spatial navigation, *Hippocampus*, pp. 740-750 (2014),
21. J. Gonzalez-Castillo, D. Handwerker, M.E. Robinson, C.W. Hoy, L.C. Buchanen, Z.S. Saad, and P.A. Bandettini, The spatial structure of resting state connectivity stability on the scale of minutes, *Frontiers in Neuroscience*, 8:138. doi:10.3389/fnins.2014.00138 (2014).
22. Z. Yang, Y. Xu, C. W. Hoy, D. A. Handwerker, G. Chen, G. Northoff, X.-N. Zuo, P. A. Bandettini, Brain Network Informed Subject Community Detection In Early-Onset Schizophrenia, *Scientific Reports*, 4 : 5549 | DOI: 10.1038/srep05549 (2014).
23. **J. Gonzalez-Castillo, C. W. Hoy, D. A. Handwerker, V. Roopchansingh, S. J. Inati, Z. S. Saad, R. W. Cox, P. A. Bandettini, Task dependence, tissue specificity and spatial distribution of widespread**

activations in large single-subject functional MRI datasets at 7T, *Cerebral Cortex*, 2014 doi:10.1093/cercor/bhu148.

24. P. Kundu, M. D. Santin, P. A. Bandettini, E. T. Bullmore, A. Petiet, Differentiating BOLD and non-BOLD signals in fMRI time series from anesthetized rats using multi-echo EPI at 11.7T, *NeuroImage*, 102, pp. 861-874 (2014).
25. R. Kaplan, D. Bush, M. Bonnefond, P. A. Bandettini, G. R. Barnes, C. F. Doeller, N. Burgess, Medial Prefrontal Theta Phase Coupling During Spatial Memory Retrieval, *Hippocampus*, 24, pp. 656-665 (2014).
26. P. A. Bandettini, Neuronal or Hemodynamic? Grappling with the functional MRI signal, *Brain Connectivity*, 4, (7), p.p. 487-498 (2014).
27. Z. Yang, Z. Huang, J. Gonzalez-Castillo, R. Dai, G. Northoff, P. Bandettini, Using fMRI to decode true thoughts independent of intention to conceal. *NeuroImage*, 99, pp. 80-92 (2014).
28. P. Wu, P. A. Bandettini, R. M. Harper, D. A. Handwerker, Effects of thoracic pressure changes on MRI signals in the brain, *Journal of Cerebral Blood Flow and Metabolism*, 35, pp. 1024-1032 (2015).
29. V. Olafsson, P. Kundu, E. C. Wong, P. A. Bandettini, T. T. Liu, Enhanced identification of BOLD-like components with multi-echo simultaneous multi-slice (MESMS) fMRI and multi-echo ICA, *NeuroImage*, 112, pp. 43-51 (2015).
30. P. Kundu, B. E. Benson, K.L. Baldwin, D. Rosen, W. M. Luh, P. A. Bandettini, D. S. Pine, M. Ernst, Robust resting state fMRI processing for studies on typical brain development based on multi-echo EPI acquisition, *Brain Imaging Behav*, 9, pp. 56-73 (2015), doi: 10.1007/s11682-014-9346-4.
31. J. W. Evans, P. Kundu, S. G. Horovitz, P. A. Bandettini, Separating slow BOLD from non-BOLD baseline drifts using multi-echo fMRI. *NeuroImage*, 105, pp. 189-197, (2015).
32. J. Gonzalez-Castillo, C. W. Hoy, D. A. Handwerker, M. E. Robinson, L. C. Buchanan, Z. S. Saad, P. A. Bandettini, Tracking ongoing cognition in individuals using brief whole-brain functional connectivity patterns. *Proc. Natl. Acad. Sci.* 12, pp. 8762-8767 (2015).
33. J. Gonzalez-Castillo, P. A. Bandettini, What cascade spreading models can teach us about the brain, *Neuron*, 86, pp. 1327-1329 (2015).
34. Z. Yang, X.-N. Zuo, K. L. McMahon, R. C. Craddock, C. Kelly, G. I. De Zubiray, I. Hickie, P. A. Bandettini, F. X. Castellanos, M. P. Milham, M. J. Wright, Genetic and Environmental Contributions to Functional Connectivity Architecture of the Human Brain, *Cerebral Cortex*, 26, pp. 2341-2352 (2016).
35. A. G. Thomas, A. Dennis, N. B. Rawlings, C. J. Stagg, L. Matthews, M. Morris, S. H. Kolind, S. Foxley, M. Jenkinson, T. Nichols, H. Dawes, P. A. Bandettini, H. Johansen-Berg, Multi-modal characterization

- of rapid anterior hippocampal volume increase associated with aerobic exercise, *NeuroImage*, 131, pp. 162-170 (2016).
36. J. Gonzalez-Castillo, G. Chen, T. Nichols, R. W. Cox, P. A. Bandettini, Variance decomposition for single-subject task-based fMRI activity estimates across many sessions. *NeuroImage*, (in press).
37. J. Gonzalez-Castillo, P. Panwar, L. C. Buchanan, C. Caballero Gaudes, D. A. Handwerker, D. C. Jangraw, V. Zachariou, S. Inati, V. Roopchansingh, P. A. Bandettini, Evaluation of multi-echo ICA denoising for task based fMRI studies: block designs, rapid event-related designs, and cardiac-gated fMRI. *NeuroImage*, (in press).

Resource Sharing and Data Sharing

We have shared data from our 100 run study (ref 12 & 26) as well as from our ongoing cortical state (ref 9) study. We plan to deposit all our data into our NIH data repository that will be started through the Data Sharing Core Facility. Until then, we will keep it in our own archives (NIH Helix Cluster) and will make available on request.

De-identified data can be shared with any researcher who signs a data use agreement as defined in NIH IRB protocol 93M0170. Data has been shared through the central.xnat.org repository and using <https://nihcesaev.cit.nih.gov> for specific requests from non-NIH researchers.

We have shared example data upon request from:

Olivia Viessmann, James Kolasisnki, FMRIB, Oxford
Rosa Panchuelo and Susan Francis, Nottingham
Gopi (Kaundiniya Gopinath) from Emory University in Atlanta
Markus Barth from Queensland
Olivier Reynaud from Lausanne

Much of our code is made available through public GitHub repositories.

Collaborations

Cesar Caballero-Gaudes - BCCBL, San Sebastian, Spain
Vince Calhoun - MIND Institute, Albuquerque, NM
Robert Cox - (Gang Cheng, Rick Reynolds, Ziad Saad) - SSCC, NIMH
Jeff Duyn - (Catie Chang), AMRI, NINDS
Mark Hallett - (Silvina Horovitz), HMC, NINDS
Demo Ivanov - Maastricht University, Maastricht, The Netherlands
Heidi Johansen-Berg - Oxford University, Oxford, UK
Alex Martin - (Steve Gotts), LBC, SCN, NIMH
Tom Nichols - University of Warwick, UK
Benedikt Poser - Maastricht University, Maastricht, The Netherlands
Kamil Uludag - Maastricht University, Maastricht, The Netherlands
Eric C. Wong - UC San Diego, CA
Leslie Ungerleider - (David Pitcher, Zachariou Valentinos), LBC, SN, NIMH
Elliot Stein - NRB, NIDA, Baltimore, MD
FMRI Core Facility - (Andy Derbyshire, Souheil Inati, Sean Marrett, Vinai Roopchansinsh)

Resources Requested

We request the following:

1. *Increased other objects budget to cover travel and purchase of equipment. (\$50K/yr). As my lab has expanded since four or even eight years ago, my annual budget has not increased concordantly to allow for increased travel and equipment expenditures.*
2. *One additional post-bac IRTA position to help support the work of my 4 post docs. An optimal combination is to have one post bac for every post doc. At the moment we have one post bac for every two post docs, which causes some strain as post bac's can be overworked and spread too thinly, and post docs may not have the assistance that they need at times.*

Bibliography

1. Biswal, B., et al., Functional Connectivity in the Motor Cortex of Resting Human Brain Using Echo-Planar Mri. *Magnetic Resonance in Medicine*, 1995. **34**(4): p. 537-541.
2. Petridou, N., et al., *Direct magnetic resonance detection of neuronal electrical activity*. *Proceedings of the National Academy of Sciences of the United States of America*, 2006. **103**(43): p. 16015-16020.
3. Thomas, A.G., et al., The effects of aerobic activity on brain structure. *Front Psychol*, 2012. **3**: p. 86.
4. Wu, P., et al., Effects of thoracic pressure changes on MRI signals in the brain. *J Cereb Blood Flow Metab*, 2015. **35**(6): p. 1024-32.
5. Birn, R.M., et al., The respiration response function: The temporal dynamics of fMRI signal fluctuations related to changes in respiration. *NeuroImage*, 2008. **40**(2): p. 644-654.
6. Thomas, A.G., et al., Multi-modal characterization of rapid anterior hippocampal volume increase associated with aerobic exercise. *Neuroimage*, 2016. **131**: p. 162-70.
7. Luh, W.M., et al., Comparison of simultaneously measured perfusion and BOLD signal increases during brain activation with T(1)-based tissue identification. *Magn Reson Med*, 2000. **44**(1): p. 137-43.
8. Kriegeskorte, N., R. Goebel, and P. Bandettini, *Information-based functional brain mapping*. *Proc Natl Acad Sci U S A*, 2006. **103**(10): p. 3863-8.
9. Gonzalez-Castillo, J., et al., Tracking ongoing cognition in individuals using brief, whole-brain functional connectivity patterns. *Proceedings of the National Academy of Sciences of the United States of America*, 2015. **112**(28): p. 8762-8767.
10. Gonzalez-Castillo, J., et al., The spatial structure of resting state connectivity stability on the scale of minutes. *Frontiers in Neuroscience*, 2014(8 JUN).
11. Handwerker, D.A., et al., Periodic changes in fMRI connectivity. *NeuroImage*, 2012. **63**(3): p. 1712-1719.
12. Gonzalez-Castillo, J., et al., Whole-brain, time-locked activation with simple tasks revealed using massive averaging and model-free analysis. *Proc Natl Acad Sci U S A*, 2012. **109**(14): p. 5487-92.
13. Murphy, K., et al., The impact of global signal regression on resting state correlations: Are anti-correlated networks introduced? *Neuroimage*, 2009. **44**(3): p. 893-905.
14. Birn, R.M., R.W. Cox, and P.A. Bandettini, Detection versus estimation in event-related fMRI: Choosing the optimal stimulus timing. *Neuroimage*, 2002. **15**(1): p. 252-264.
15. Birn, R.M., R.W. Cox, and P.A. Bandettini, Experimental designs and processing strategies for fMRI studies involving overt verbal responses. *Neuroimage*, 2004. **23**(3): p. 1046-1058.
16. Birn, R.M. and P.A. Bandettini, The effect of stimulus duty cycle and "off" duration on BOLD response linearity. *Neuroimage*, 2005. **27**(1): p. 70-82.
17. Bellgowan, P.S.F., Z.S. Saad, and P.A. Bandettini, Understanding neural system dynamics through task modulation and measurement of functional MRI amplitude, latency, and width. *Proceedings of the National Academy of Sciences of the United States of America*, 2003. **100**(3): p. 1415-1419.
18. Kundu, P., et al., Differentiating BOLD and non-BOLD signals in fMRI time series using multi-echo EPI. *Neuroimage*, 2012. **60**(3): p. 1759-70.

19. Kundu, P., et al., Integrated strategy for improving functional connectivity mapping using multiecho fMRI. *Proc Natl Acad Sci U S A*, 2013. **110**(40): p. 16187-92.
20. Wong, E.C., Direct imaging of functional networks. *Brain Connect*, 2014. **4**(7): p. 481-6.
21. Guimaraes, A.R., et al., Imaging subcortical auditory activity in humans. *Human Brain Mapping*, 1998. **6**(1): p. 33-41.
22. Beissner, F., et al., Dual-echo EPI for non-equilibrium fMRI - implications of different echo combinations and masking procedures. *Neuroimage*, 2010. **52**(2): p. 524-31.
23. Poser, B.A., et al., BOLD contrast sensitivity enhancement and artifact reduction with multiecho EPI: Parallel-acquired inhomogeneity-desensitized fMRI. *Magnetic Resonance in Medicine*, 2006. **55**(6): p. 1227-1235.
24. Craddock, R.C., et al., A whole brain fMRI atlas generated via spatially constrained spectral clustering. *Hum Brain Mapp*, 2012. **33**(8): p. 1914-28.
25. Smith, S.M., et al., Correspondence of the brain's functional architecture during activation and rest. *Proc Natl Acad Sci U S A*, 2009. **106**(31): p. 13040-5.
26. Gonzalez-Castillo, J., et al., Task Dependence, Tissue Specificity, and Spatial Distribution of Widespread Activations in Large Single-Subject Functional MRI Datasets at 7T. *Cereb Cortex*, 2015. **25**(12): p. 4667-77.
27. Evans, J.W., et al., Separating slow BOLD from non-BOLD baseline drifts using multi-echo fMRI. *Neuroimage*, 2015. **105**: p. 189-97.
28. Lu, H. and P.C.M. van Zijl, A review of the development of Vascular-Space-Occupancy (VASO) fMRI. *NeuroImage*, 2012. **62**(2): p. 736-742.
29. Felleman, D.J. and D.C. Van Essen, Distributed hierarchical processing in the primate cerebral cortex. *Cereb Cortex*, 1991. **1**(1): p. 1-47.
30. Hasson, U., et al., Intersubject synchronization of cortical activity during natural vision. *Science*, 2004. **303**(5664): p. 1634-1640.
31. Huber, L., et al., Functional cerebral blood volume mapping with simultaneous multi-slice acquisition. *Neuroimage*, 2016. **125**: p. 1159-68.